Drug Design, Development and Therapy

Dovepress
open access to scientific and medical research

Open Access Full Text Article

ORIGINAL RESEARCH

Epigallocatechin-3-gallate enhances the osteoblastogenic differentiation of human adipose-derived stem cells

This article was published in the following Dove Medical Press journal:
Drug Design, Development and Therapy

Jing Zhang,[1] Kai Wu,[2] Ting Xu,[3] Jiajun Wu,[1] Pengfei Li,[1] Hong Wang,[4] Huiling Wu,[1] Gang Wu[5]

[1]Department of Plastic and Aesthetic Center, The First Affiliated Hospital of Zhejiang University, Hangzhou, Zhejiang, China; [2]Spine Lab, Department of Orthopedic Surgery, The First Affiliated Hospital of Zhejiang University, Hangzhou, Zhejiang, China; [3]Department of Stomatology, First Affiliated Hospital, Zhejiang University, Hangzhou, China; [4]Department of Oral and Maxillofacial Surgery, Amsterdam University Medical Centre, University of Amsterdam and Vrije Universiteit Amsterdam, Amsterdam, North Holland, the Netherlands; [5]Department of Oral Implantology and Prosthetic Dentistry, Academic Centre for Dentistry Amsterdam, University of Amsterdam and Vrije Universiteit Amsterdam, Amsterdam, North Holland, the Netherlands

Correspondence: Huiling Wu
Department of Plastic and Aesthetic Center, The First Affiliated Hospital of Zhejiang University, Hangzhou, Qingchun Road 79, Hangzhou 310003, China
Tel +86 571 8723 5018
Fax +86 571 8707 2577
Email zywhl@zju.edu.cn

Gang Wu
Department of Oral Implantology and Prosthetic Dentistry, Academic Centre for Dentistry Amsterdam, University of Amsterdam and Vrije Universiteit Amsterdam, Gustav Mahlerlaan 3004, 1081LA Amsterdam, the Netherlands
Tel +31 20 598 0866
Fax +31 20 598 0333
Email g.wu@acta.nl

Purpose: The aim of this study is to investigate the effects of epigallocatechin-3-gallate (EGCG), a major polyphenol extracted from green tea, on the osteoblastogenic differentiation of human adipose-derived stem cells (hASCs).

Patients and methods: hASCs were acquired from human adipose tissue. With informed consent, subcutaneous adipose tissue samples were harvested from periorbital fat pad resections from ten healthy female adults who underwent double eyelid surgery. hASCs were cultured in osteogenic medium with or without EGCG (1 μM, 5 μM, or 10 μM) for 14 days. We evaluated the effects of EGCG by quantifying cell growth, ALP activity (an early osteoblastogenic differentiation marker), BSP, OCN (a late osteoblastogenic differentiation marker), and extracellular matrix mineralization. We also performed Western blots to measure osteoblastogenesis-related proteins such as Runx2 and adipoblastogenesis-related transcription factors, such as STAT3, C/EBP-α, and PPAR-γ.

Results: EGCG at 5 μM resulted in significantly higher cell proliferation and ALP activity than did the control on days 3, 7, and 14. On day 7, 5 μM EGCG significantly enhanced BSP expression. On day 14, EGCG at all concentrations promoted OCN expression. In addition, EGCG at 5 μM resulted in the highest level of extracellular matrix mineralization. On day 3, the expression levels of Runx2 were significantly higher in the 5 μM EGCG group than in the other groups, whereas later, on days 7 and 14, Runx2 expression levels in the EGCG group were significantly lower than those of the control group. EGCG at all three concentrations was associated with significantly lower levels of phosphorylated STAT3, C/EBP-α, and PPAR-γ.

Conclusion: EGCG at 5 μM significantly enhanced the osteoblastogenic differentiation of hASCs.

Keywords: EGCG, hASCs, osteoblastogenesis, STAT3, bone regeneration

Introduction

Large-volume bone defects (LVBD) can result from congenital nonunion, trauma, inflammation, or osteosarcoma resection and can severely impair esthetics and musculoskeletal function.[1] It remains highly challenging to repair LVBD in the field of orthopedics and maxillofacial surgery. It has been reported that 5%–10% of all fractures are associated with impaired healing, resulting in delayed union or nonunion.[2–4] How to repair large bone defect remains an important clinical problem, and none of the approaches proposed to date have proven to be very effective.[5] LVBD may require bone grafting to fill defects and provide support. Autologous bone grafting is regarded the gold-standard treatment option for LVBD due to its osteoconductive,

osteoinductive, and osteogenic characteristics.[6] However, its use is limited by insufficient availability, donor-site pain and morbidity, and varied resorption rates.[7] The conventional alternatives to autologous bone grafting, including allografting and xenografting, cannot heal LVBD because they lack either osteogenic cells or osteoinductive growth factors. In the clinic, autologous bone grafting remains indispensable to compensate for these shortages in alternative grafts. In these cases, the abovementioned limitations of autologous bone grafting remain.

In recent years, cell-based tissue engineering has shown promise for application potential in bone regeneration.[8] Bone marrow-derived stem cells (BMSCs) were originally considered to be the primary cell resource for bone tissue engineering.[9] However, the application of BMSCs is associated with several disadvantages, such as donor-site pain and low cell output, leading to sustained efforts to search for alternative cells.[10] Human adipose-derived stem cells (hASCs) are highly promising because of their greatly increased accessibility, higher yield efficiency, less painful harvest procedures, and lower donor-site morbidity when compared with BMSCs.[11] Furthermore, hASCs proliferate more rapidly[12] and enter senescence in later passages than do BMSCs.[13]

On the other hand, although hASCs exhibit multipotency as do other mesenchymal stem cells (MSCs), they also show a native tendency toward adipogenic differentiation. The activation of PPAR-γ, a key gene for adipogenic differentiation, not only promotes adipogenesis but also downregulates the expression of Runx2 and interferes with its transactivation ability, thereby suppressing osteogenic differentiation. Consequently, the osteogenic commitment of hASCs is more complicated than that of BMSCs and requires both suppression of its adipogenic differentiation and enhancement of its osteogenic differentiation. One way to facilitate osteogenesis in hASCs is to add osteogenic agents.[14,15] However, it has been shown that the responses of hASCs to bone morphogenetic protein 2 (BMP-2), a well-established osteoinductive growth factor, are highly unpredictable and largely donor-dependent.[1,16–18] Therefore, sustained efforts have been made to seek effective agents to induce the osteogenic differentiation of hASCs in vitro.

Green tea is one of the most popular beverages in the world, with well-recognized benefits to health. Habitual tea drinking may reduce the risk of hip fractures[19,20] and may help to retain bone mineral density (BMD) in postmenopausal women.[21] In line with the beneficial effects of green tea, epigallocatechin-3-gallate (EGCG), the most abundant polyphenol in green tea,[22] shows various beneficial effects, such as antioxidant, anti-inflammatory, anticancer, and antiatherogenic effects.[23–25] Such effects of EGCG may be associated with the activation of genes and signaling pathways, such as the mitogen-activated protein kinase (MAPK)-dependent pathway and the ubiquitin/proteasome degradation pathway.[22,26,27] EGCG was shown to enhance the osteogenesis of BMSCs and osteoblast-like cells[28,29] and to inhibit the adipogenesis of preadipocytes.[30] However, there has been no direct experimental evidence identifying EGCG's effects on osteogenic differentiation in hASCs.

In this study, we aimed to investigate the effects of EGCG at different concentrations on the osteogenic and adipogenic differentiation of hASCs and to explore the application potential of EGCG in hASC-based bone tissue engineering.

Materials and methods

Adipose tissue donors

After obtaining informed consent, subcutaneous adipose tissue samples were harvested from periorbital fat pad resections from ten healthy female adults (age range: 25–35 years, mean: 30 years) who underwent double eyelid surgery (the First Affiliated Hospital, Zhejiang University, Hangzhou, China). We obtained approval from the institutional review board (IRB). All participants were well-informed of the purpose and each submitted written informed consent before participating in the study. This study was conducted in accordance with the Declaration of Helsinki.

hASC isolation and preparation

To isolate hASCs, adipose tissue was cut into 1 mm^3 pieces and undesirable components, such as vascular cells and connective tissues, were eliminated. The 1 mm^3 adipose tissue was enzymatically digested with 0.1% collagenase A (Sigma-Aldrich Co., St Louis, MO, USA) in DMEM (Corning Incorporated, Corning, NY, USA) under continuous shaking conditions for 30 min at 37°C. Cells were then suspended in DMEM with 100 U/mL penicillin, 100 µg/mL streptomycin (Sigma-Aldrich Co.), 10% FBS (Thermo Fisher Scientific, Waltham, MA, USA), and 2 mM L-glutamine. This was followed by centrifugation at 1,200 rpm for 4 min. The cell-containing interface was harvested and cultured in DMEM with 100 U/mL penicillin, 100 µg/mL streptomycin (Sigma-Aldrich Co.), 10% FBS (Thermo Fisher Scientific), and 2 mM L-glutamine (Sigma-Aldrich Co.). Cells were then seeded at a density of $2\times10^4/cm^2$ into overturned culture flasks in a 5% CO_2 incubator at 37°C. The medium was refreshed every 3 days. When nearly 80% confluent, hASCs were harvested by adding 0.25% trypsin (Thermo Fisher Scientific). In all experiments, hASCs at passage 4 were used. The phenotype profile of hASCs (passage 4) was evaluated through flow cytometry analysis using PE-labeled cluster

designation CD29, CD31, CD44, CD45, CD73, CD90, and CD105 antibodies (data not shown).[31,32]

hASCs were seeded in DMEM with 100 U/mL penicillin, 100 μg/mL streptomycin, 10% FBS, and 2 mM L-glutamine. When 60%–70% confluence was reached, we replaced the medium with osteogenic differentiation medium (basal culture medium plus ascorbate, β-glycerophosphate, and dexamethasone as supplements) (HUXMD-90021; Cyagen Biosciences Inc, Guangzhou, China) with vehicle (0.1% PBS) or with EGCG at different concentrations (1 μM, 5 μM, or 10 μM). The medium was refreshed every 3 days until the end of the culture period.

Cell growth assay

Cell growth was analyzed using a cell counting kit-8 (CCK-8; Dojindo Co., Kumamoto, Japan). Briefly, hASC cells were planted in 96-well plates (5,000 cells per cm^2) and incubated at 37°C in a 5% CO_2 humidified atmosphere for 24 h. Then, the cells were divided into four groups and were treated with EGCG (0 μM, 1 μM, 5 μM, or 10 μM). After the treatment, the cells were first washed with PBS and then with 100 μL DMEM. Ten microliters of CCK-8 solution was added to each well; the plates were then incubated for one more hour. The absorbance was measured by a microplate reader at a wavelength of 450 nm to count the number of viable cells.

ALP staining and quantification

The hASCs were seeded in six-well plates and cultured in EGCG at varying concentrations (0 μM, 1 μM, 5 μM, or 10 μM). On day 14, ALP staining was carried out using a BCIP/NBT Alkaline Phosphatase Color Development Kit (Beyotime, Shanghai, China). Briefly, the cells were fixed with 4% paraformaldehyde and then incubated in a mixture of nitro-blue tetrazolium and 5-bromo-4-chloro-3-indolyl-phosphate. The ALP staining was observed under an optical microscope (Olympus IX71; Olympus Corporation, Tokyo, Japan). Culture medium was collected after 3 days, 7 days, and 14 days. This was followed by centrifugation at 1,000 rpm for 10 min. The supernatants were harvested and then tested. The quantification of ALP activity was determined using an Alkaline Phosphatase Detection Kit (Nanjing Jiancheng Bioengineering Institute, Nanjing, China).

Mineralization

Matrix mineralization was analyzed by Alizarin red staining (ARS). hASCs were fixed in 4% paraformaldehyde for 30 min and rinsed with PBS before staining. To detect calcium deposits, hASCs were stained with Alizarin red (40 mM, pH 4.2; Cyagen) for 3–5 min and then rinsed twice with PBS. Subsequently, an inverted microscope was used to visualize staining. Bright red nodules showed mineralized matrix deposition that indicated osteoblastogenic differentiation of hASCs. The area of mineralization was calculated using software ImageJ.

Western blotting

Primary antibodies against osteocalcin (OCN; Sigma-Aldrich Co., catalog number: SAB1306277), bone sialoprotein (BSP, diluted 1:1,000; Cell Signaling Technology, Boston, MA, USA; catalog number 5468S), Runx2 (diluted 1:1,000; Cell Signaling Technology; catalog number 8486), STAT3 (diluted 1:1,000; Cell Signaling Technology; catalog number 9139), pSTAT3 (diluted 1:2,000; Cell Signaling Technology; catalog number 9145), PPAR-γ (diluted 1:1,000; Cell Signaling Technology; catalog number 2435), C/EBP-α (diluted 1:1,000; Cell Signaling Technology; catalog number 8178), and β-actin (diluted 1:1,000; Cell Signaling Technology; catalog number 4970) were incubated with the blots at 4°C overnight. Horseradish peroxidase-conjugated anti-rabbit or anti-mouse secondary antibodies (Cell Signaling Technology) were used as secondary antibodies at a dilution of 1:10,000 and incubated at room temperature for 1 h.

Statistical analysis

All results were presented as mean ± SD for at least three independent experiments. Differences among groups were analyzed by ANOVA (for experiments with more than two groups). A two-tailed value of $p<0.05$ was considered to be statistically significant. Statistical analysis was performed using GraphPad Prism 6 (GraphPad Software, Inc., La Jolla, CA, USA).

Results

Effect of EGCG on the growth of hASCs

On day 3, EGCG at 5 μM but not at 1 μM or 10 μM resulted in significantly higher cell viability than did the control (without EGCG) (Figure 1). On day 7, EGCG at all concentrations significantly enhanced cell viability as compared to the control. On day 14, 5 μM EGCG induced significantly higher cell viability than did the control, whereas 1 μM or 10 μM EGCG did not. Among these three different concentrations, 5 μM EGCG showed a consistent ability to promote cell viability in hASCs.

Effect of EGCG on osteoblastogenic differentiation of hASCs

EGCG at 5 μM strongly promoted ALP expression of hASCs when compared to the control group on day 14 (Figure 2A).

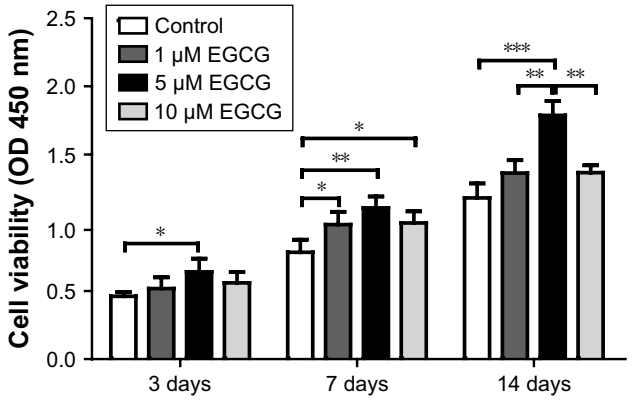

Figure 1 CCK-8 was used to analyze cell proliferation of hASCs at various concentrations of EGCG.
Notes: Cell growth in EGCG groups was higher than in the control group on days 3, 7, and 14; 5 μM was optimal to enhance cell proliferation. All data are presented as mean and SD. *$p<0.05$; **$p<0.01$; and ***$p<0.001$ (N=4).
Abbreviations: CCK-8, cell counting kit-8; EGCG, epigallocatechin-3-gallate; hASCs, human adipose-derived stem cells.

ALP activity quantification assay showed that 5 μM EGCG significantly promoted ALP activity on all the time points, whereas 1 μM and 10 μM EGCG did so on days 3 and 14 but not on day 7 (Figure 2B).

After 7 days, 5 μM EGCG significantly enhanced the expression of BSP, whereas EGCG at 1 μM and 10 μM had no significant effect on BSP expression when compared to the control (Figure 3A and B). Western blot analysis showed that 1 μM and 10 μM EGCG resulted in significantly higher expression of OCN in hASCs on day 14 (Figure 3C and D). OCN expression at 5 μM EGCG was higher than that of the control on day 14. At the same time point, 5 μM and 10 μM EGCG significantly promoted extracellular mineralization, whereas 1 μM EGCG had no significant effect when compared to the control (Figure 4). All these results showed that 5 μM EGCG was optimal for inducing osteoblastogenic differentiation of hASCs.

Effect of EGCG on the expression of osteoblastogenic and adipoblastogenic transcription factors

After 3 days of culture, the level of Runx2 expression in 5 μM EGCG was significantly higher when compared to the other groups (Figure 5A and B). On day 7, Runx2 expression in 5 μM EGCG was significantly downregulated, and in the other two EGCG groups, Runx2 expression levels were lower than those of the control (Figure 5C and D). On day 14, EGCG at all three concentrations was associated with significantly lower levels of Runx2 expression when compared to the control (Figure 5E and F).

On days 3 and 14, EGCG at all concentrations significantly downregulated the expression of PPAR-γ in comparison with the control (Figure 6A, B, E, and F). On day 7, 5 μM EGCG significantly suppressed the expression of PPAR-γ (Figure 6C and D). EGCG at 5 μM showed the most efficacy to suppress PPAR-γ expression. The level of C/EBP-α expression in all EGCG groups was significantly lower than that of the control on day 14 (Figure 7). Compared to the concentrations of 1 μM and 10 μM, EGCG at 5 μM exhibited stable and consistent ability in downregulating PPAR-γ and C/EBP-α expression.

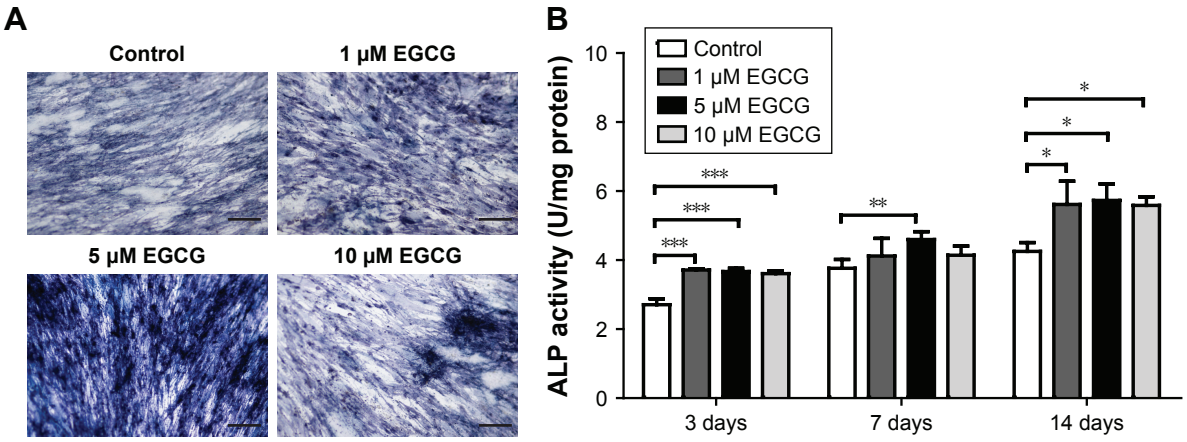

Figure 2 Effects of EGCG on ALP activity.
Notes: (**A**) Dose effect of EGCG on ALP staining in hASCs was determined under osteogenic induction on day 14. The ALP staining method revealed that the number of ALP-positive cells was increased by EGCG. ALP staining in the 5 μM EGCG group was strongest among all EGCG groups. (**B**) The ALP activity of hASCs for all groups at various time points was quantitatively analyzed. Compared to the control group, ALP activity was strengthened by EGCG through the whole period (days 3, 7, and 14). All data are presented as mean and SD. *$p<0.05$; **$p<0.01$; and ***$p<0.001$ (N=5). Bar=200 μM.
Abbreviations: EGCG, epigallocatechin-3-gallate; hASCs, human adipose-derived stem cells.

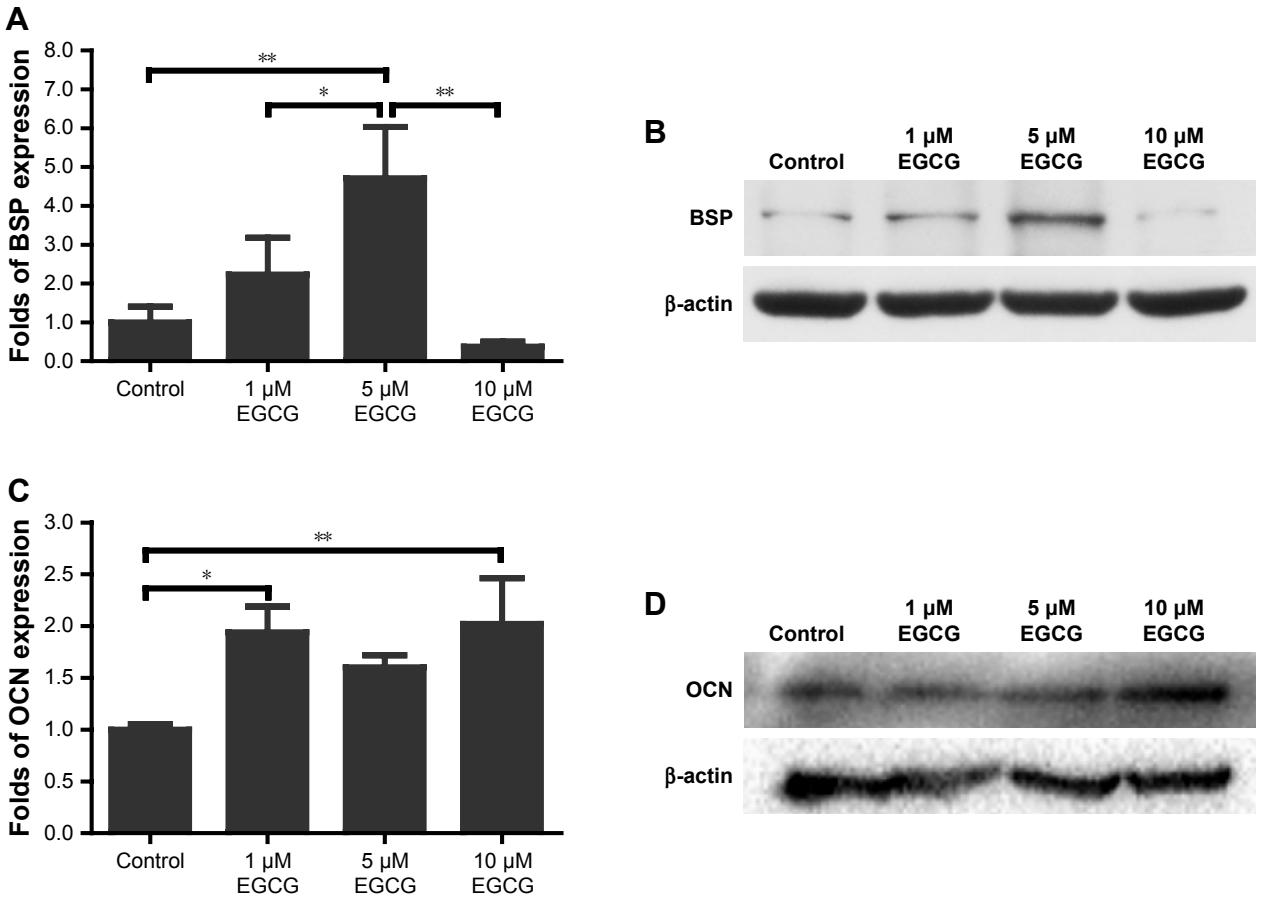

Figure 3 Western blotting was used to analyze the expression of osteogenic genes BSP and OCN in hASCs cultured at various concentrations of EGCG for 7 days and 14 days.

Notes: (**A**) The level of BSP was significantly promoted in the 5 μM EGCG group. (**B**) BSP mRNA expression of osteogenic induction on day 7. (**C**) The level of OCN was strengthened in the EGCG groups. (**D**) OCN mRNA expression at day 14 of osteogenic induction. All data are presented as mean and SD. *$p<0.05$; **$p<0.01$ (N=3).

Abbreviations: BSP, bone sialoprotein; EGCG, epigallocatechin-3-gallate; hASCs, human adipose-derived stem cells; OCN, osteocalcin.

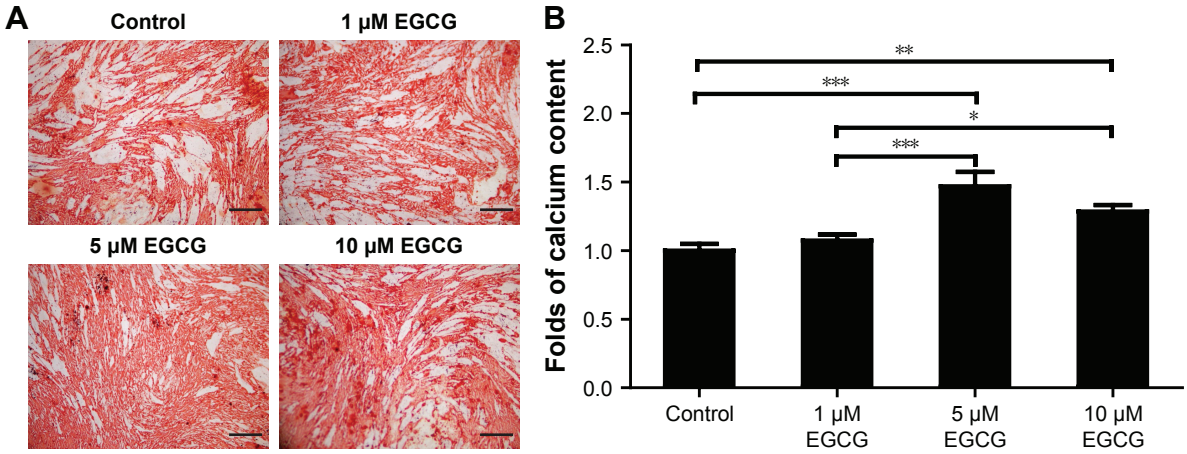

Figure 4 Effect of EGCG on mineralization.

Notes: (**A**) Dose effect of EGCG on matrix mineralization in hASCs was determined under osteogenic induction conditions on day 14 by ARS. ARS in the 5 μM EGCG group was much stronger than in the other groups. (**B**) Mineralization was quantitatively analyzed. The calcium content in the 5 μM EGCG group was 1.47 times greater than that of the control group. In the 10 μM EGCG group, the calcium content was 1.29-fold greater than that of the control group. All data are presented as mean and SD. *$p<0.05$, **$p<0.01$ and ***$p<0.001$ (N=3). Bar=200 μM.

Abbreviations: ARS, Alizarin red staining; EGCG, epigallocatechin-3-gallate; hASCs, human adipose-derived stem cells.

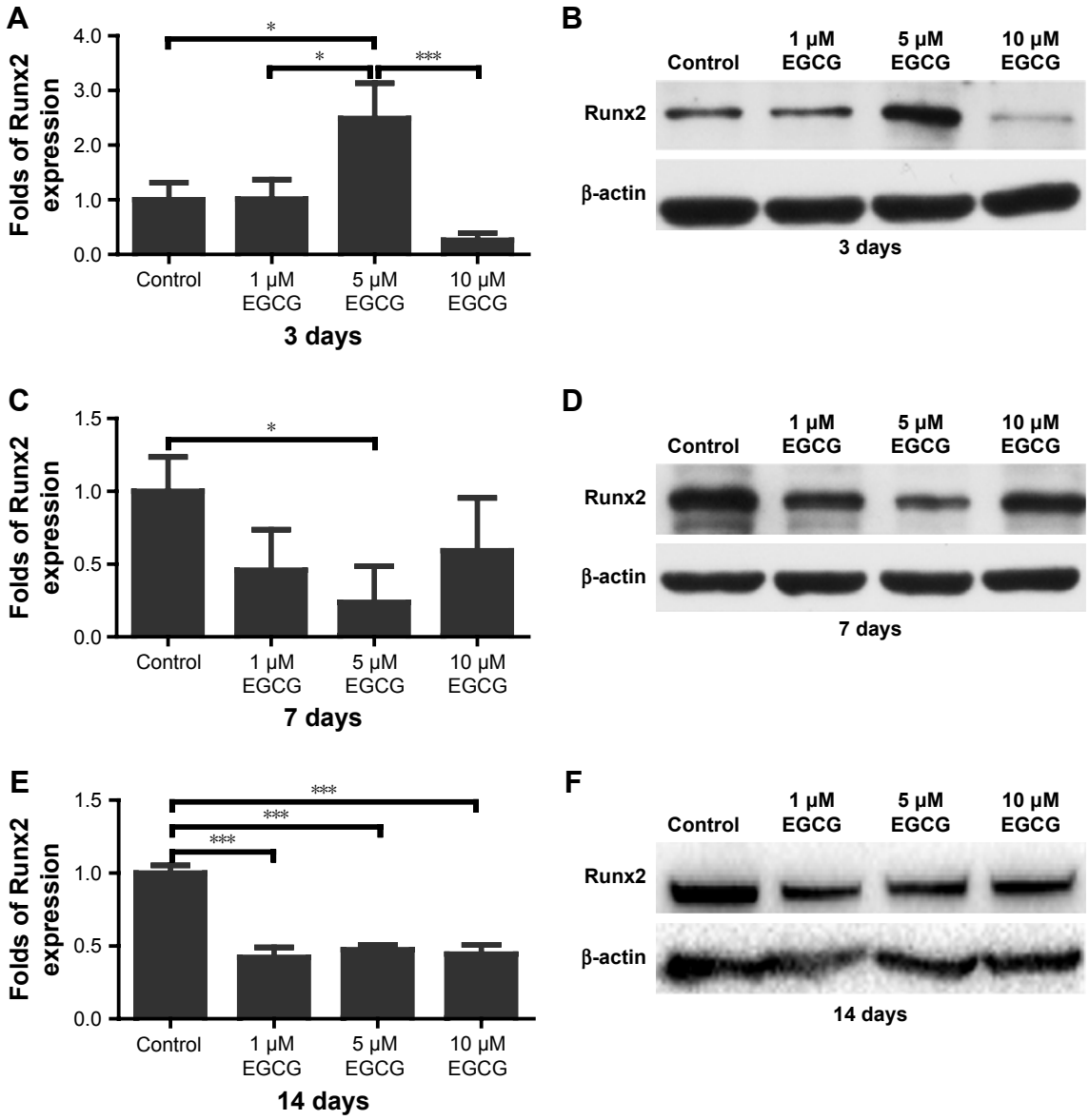

Figure 5 Western blotting was used to analyze the expression of osteogenic genes Runx2 in hASCs cultured in various concentrations of EGCG for 14 days.
Notes: (**A**) The level of Runx2 in the 5 μM EGCG group was significantly higher than that of the control and other EGCG groups. (**B**) Runx2 mRNA expression at day 3 of osteogenic induction. (**C**) On day 7, Runx2 expression was significantly downregulated in the 5 μM EGCG group. (**D**) Runx2 mRNA expression at day 7 of osteogenic induction. (**E**) The levels of Runx2 in EGCG groups were significantly lower than those in the control group on day 14. (**F**) Runx2 mRNA expression on day 14 of osteogenic induction. All data are presented as mean and SD. *$p<0.05$; ***$p<0.001$ (N=3).
Abbreviations: EGCG, epigallocatechin-3-gallate; hASCs, human adipose-derived stem cells.

Five and 10 μM EGCG significantly downregulated expression levels of phosphorylated STAT3 but promoted unphosphorylated STAT3 on day 14 (Figure 8). The expression levels of *p*-STAT3 and STAT3 in 1 μM were not significantly different from those of control. The concentration of 5 μM demonstrated the highest potential to restrict expression of *p*-STAT3.

Discussion

Cell-based bone tissue engineering is an interdisciplinary technology that combines stem cells and technologies in material engineering and bioactive reagents with the ultimate goal of regenerating bone tissues in LVBD.[14,33,34] For hASC-based tissue-engineered bone, the application of bioactive agents to efficaciously induce the osteoblastogenic differentiation of hASCs is pivotal for the success of this technique. One attractive group of such bioactive agents are monomers extracted from plants. Previous studies showed that EGCG, the main component of the tea polyphenols, promoted the osteogenic differentiation of BMSCs[28,29] and human primary dedifferentiated fat cells.[35] In this study, for the first time, we showed that EGCG significantly promoted the proliferation

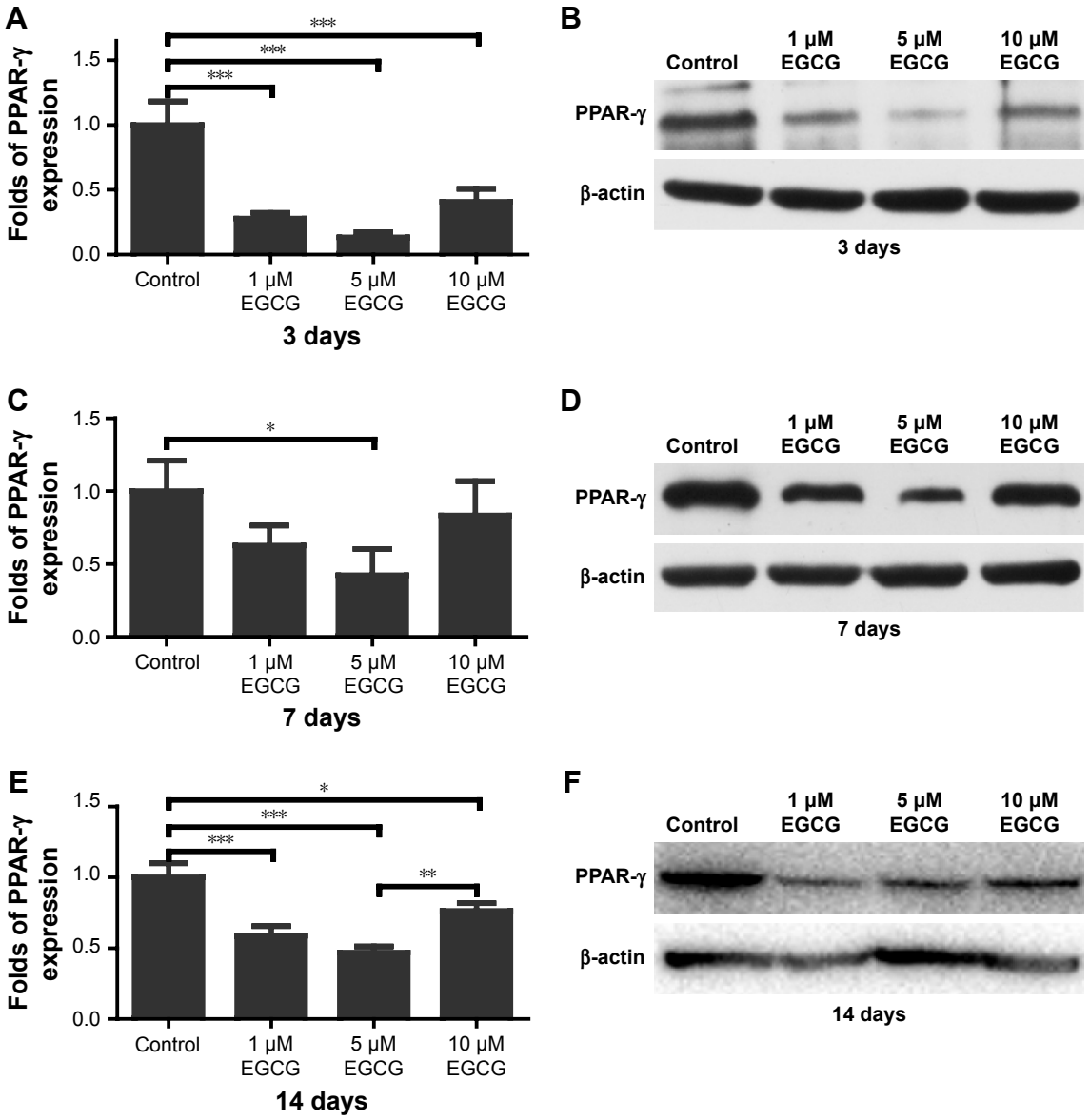

Figure 6 Western blotting was used to analyze the expression of adipogenic genes PPAR-γ in hASCs cultured in various concentrations of EGCG for 14 days. EGCG suppressed the expression of PPAR-γ, and 5 μM was optimal for suppressing PPAR-γ expression.

Notes: (**A**) On day 3, EGCG at all concentrations significantly suppressed PPAR-γ expression. (**B**) PPAR-γ expression at day 3 of osteogenic induction. (**C**) On day 7, EGCG at 5 μM significantly downregulated PPAR-γ expression. (**D**) PPAR-γ expression at day 7 of osteogenic induction. (**E**) EGCG at all concentrations significantly suppressed PPAR-γ expression on day 14, and the expression level in the 5 μM EGCG group was lowest. (**F**) PPAR-γ mRNA expression at day 14 of osteogenic induction. All data are presented as mean and SD. *$p<0.05$; **$p<0.01$; and ***$p<0.001$ (N=3).

Abbreviations: EGCG, epigallocatechin-3-gallate; hASCs, human adipose-derived stem cells.

and osteoblastogenic differentiation of hASCs, thereby showing promising application potential.

The BMP family belongs to the superfamily of TGF-beta (TGF-β). The typical role of BMPs is to induce cartilage and bone formation. The ability of exogenous BMPs to promote osteogenic differentiation of hASCs in vitro is highly dependent on several factors, such as BMP type, concentration, differentiation medium, and administration time point.[36–38] To achieve optimal osteoinductive efficacy, BMPs need to be gradually delivered to the target site at low levels and in a sustained manner rather than in a single, high-dose burst.[39] Although BMPs have been reported to promote both osteogenic and adipogenic differentiation of many other MSCs, their effect on the osteogenic commitment of hASCs remains uncertain and controversial.[1] A potential mechanism is that BMP alone can simultaneously activate and induce osteogenic or adipogenic signaling in different cells of one hASC pool that is highly dependent on the epigenetic status of hASCs.[1] Both signaling pathways antagonize one another through different signaling levels. The mutual suppression

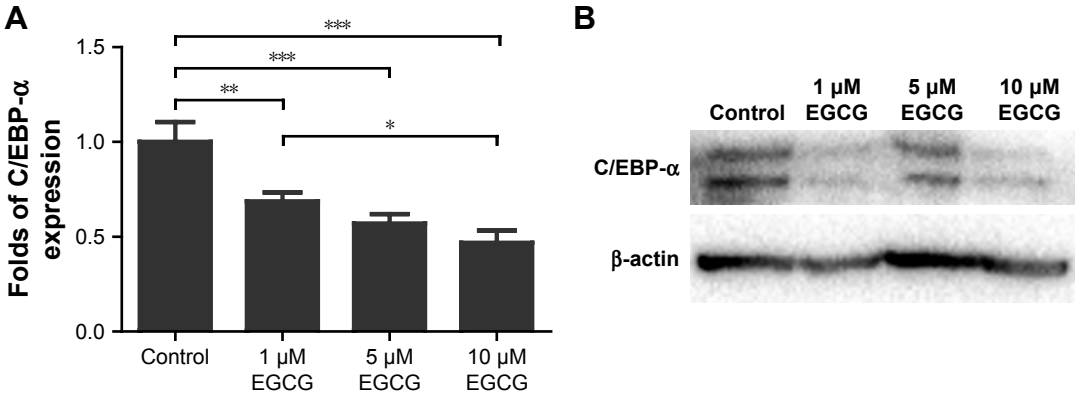

Figure 7 Western blotting was used to analyze the expression of adipogenic genes C/EBP-α in hASCs cultured in various concentrations of EGCG for 14 days.
Notes: (**A**) EGCG at all concentrations significantly suppressed the expression of C/EBP-α at day 14. The level of C/EBP-α expression was lowest in 10 μM EGCG. (**B**) C/EBP-α expression at day 14 of osteogenic induction. All data are presented as mean and SD. *$p<0.05$; **$p<0.01$; and ***$p<0.001$ (N=3).
Abbreviations: EGCG, epigallocatechin-3-gallate; hASCs, human adipose-derived stem cells.

and inhibition between these two signaling pathways result in a noncommitment stage. Unlike BMPs, we showed that EGCG not only promoted the osteogenic differentiation but also suppressed the adipogenic differentiation of hASCs, suggesting a promising application of EGCG in hASC-based bone tissue engineering.

In this study, we used three concentrations of EGCG, namely, 1 μM, 5 μM, and 10 μM, to investigate the effects of EGCG on the osteoblastogenic differentiation of hASCs. Cell viability in the 5 μM EGCG group showed the highest levels on days 3, 7, and 14. Compared to 5 μM EGCG, higher doses of EGCG, eg, 10 μM, did not enhance cell viability, which had similar levels to those of 1 μM EGCG. This result suggested that EGCG supports cell proliferation in a dose-dependent manner. EGCG, a potent antioxidant, plays a major role in reducing levels of excessive ROS,[40] which are well-known to be deleterious. However, a suitable EGCG dosage might maintain ROS at favorable levels to benefit cell proliferation and growth, as a basal level of ROS is considered necessary for many cellular functions. Several previous studies suggested that EGCG ranging from 1 μM to 10 μM promotes cell proliferation.[41,42] The result of Jin et al's[43] work showed that EGCG at 2.5 μM and 5 μM maximally enhanced the proliferation of human BMSCs, which is consistent with the findings in the present study. However, the molecular mechanisms of EGCG promoting hASCs proliferation in a dose-dependent manner remain unclear and require further study. ALP, an early osteoblastogenic differentiation marker, was activated to higher levels in the EGCG groups when compared to the control group on days 3 and 14. EGCG at 5 μM exhibited a consistent effect of significantly inducing higher levels of ALP activity at all time points (Figure 2), in agreement with results from Jin et al's[43] work, to the effect that 5 μM EGCG maximally elevated ALP activity in human BMSCs. BSP expression on day 7 was significantly promoted by 5 μM EGCG, also in accordance with the results of Jin et al.[43] On day 14, the level of mineralization in the 5 μM EGCG group

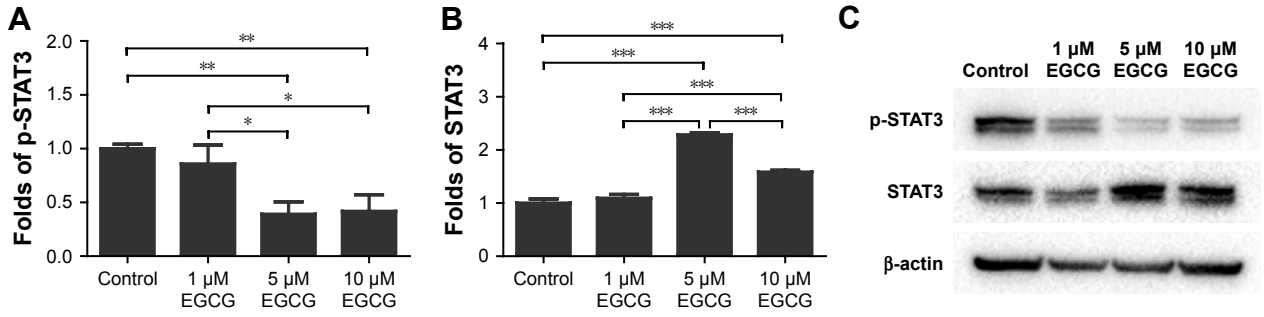

Figure 8 Western blotting was used to analyze the expression of p-STAT3 (**A**) and STAT3 (**B**) in hASCs cultured in various concentrations of EGCG for 14 days.
Notes: Compared to the control group, EGCG with the concentration of 5 μM and 10 μM decreased the phosphorylation of STAT3. (**C**) p-STAT3 and STAT3 mRNA expression at day 14 of osteogenic induction. All data are presented as mean and SD. *$p<0.05$; **$p<0.01$; and ***$p<0.001$ (N=3).
Abbreviations: EGCG, epigallocatechin-3-gallate; hASCs, human adipose-derived stem cells.

was the highest in comparison with other groups (Figure 4). In previous studies, the optimal concentration to induce the mineralization of human BMSCs[43] and human osteoblast-like cells[44] was found to be 5 μM, which was consistent with our result for hASCs. Five micromolar EGCG was associated with significantly higher Runx2 expression in the early stage of osteoblastogenic differentiation and lower PPAR-γ and *p*-STAT3 expression when compared to the 1 μM and 10 μM EGCG groups, possibly indicating that osteodifferentiation in the 5 μM EGCG group was significantly higher.

Runx2 plays several roles throughout the process of osteoblastogenesis.[45] It is an essential transcription factor that controls skeletal development by regulating the differentiation of osteoblasts and the expression of many extracellular matrix protein genes during osteoblast differentiation.[46,47] Consistently, previous studies showed that EGCG significantly elevated expression levels of Runx2 gene at early time points, eg, 24–48 h.[28,35] During osteoblast differentiation, Runx2 upregulates the expression of bone matrix protein genes, including Col1a1, Spp1, Ibsp, Bglap, and Fn1, in vitro and activates many promoters, including those of Col1a1, Col1a2, Spp1, BGLAP, and Mmp13.[48] In contrast, in the maturation stage, Runx2 should be downregulated to further support osteoblast maturation and to form mature bone.[49] The effects of EGCG on early upregulation and subsequent downregulation of Runx2 might be beneficial to the entire process of osteogenic differentiation. In our study, we found that Runx2 expression with 5 μM EGCG on day 3 (early osteoblastogenic differentiation stage) was significantly higher than that of the control and EGCG at 1 μM and 10 μM. This finding suggested that 5 μM EGCG bore a significantly higher capacity to initiate osteoblastogenic differentiation than EGCG at other concentrations. The Runx2 levels gradually decreased with time. On day 14, Runx2 expression levels (final osteoblastogenic differentiation stage) in all three EGCG groups were significantly lower than those of the control group (Figure 5E). Such a downregulation of Runx2 might be associated with the progress of osteoblastic differentiation and maturation.[49]

Since hASCs have an intrinsic tendency toward adipogenic differentiation,[50] the osteogenic commitment of hASCs requires both suppression of adipogenic differentiation and the enhancement of osteogenic differentiation.[51] Adipogenesis is a tightly controlled process that involves an intricate network of transcription factors acting at different time points during differentiation.[52] Several studies have clearly established PPAR-γ as a key regulator of adipocyte development both in vitro and in vivo. This receptor is known to be obligatory for adipocyte differentiation and is, in many cases, sufficient to convert non-adipose cells to adipocyte-like cells.[53] C/EBP-α is expressed late in adipogenesis and is a key regulator of adipocyte differentiation.[54] The relative importance of PPAR-γ and C/EBP-α in adipogenesis has been investigated, and the results showed that PPAR-γ can induce adipogenesis in C/EBP-$\alpha^{-/-}$ mouse embryonic fibroblasts in vitro, whereas C/EBP-α is unable to do the same in PPAR-$\gamma^{-/-}$ mouse embryonic fibroblasts.[55] These results confirm the leading role of PPAR-γ in adipocyte differentiation and indicate that C/EBP-α is not obligatory for activation of adipocyte-specific genes, provided PPAR-γ is ectopically expressed.[55] We investigated the effect of EGCG on adipogenic differentiation by evaluating these two critical transcription factors: PPAR-γ and C/EBP-α. Tang et al[56] found that EGCG from 10 μg/mL to 25 μg/mL significantly downregulated the expression of PPAR-γ and C/EBP-α in 3T3-L1 adipocytes. Consistent with their findings, our results demonstrated that EGCG significantly suppressed the expression of both PPAR-γ and C/EBP-α in hASCs in a dose-dependent manner; PPAR-γ expression levels were lowest at 5 μM EGCG compared to those in other EGCG groups (Figure 6). Therefore, it can be concluded that EGCG, in addition to promoting osteogenic differentiation, can significantly suppress the adipogenic differentiation of hASCs (Figures 6 and 7).

The STAT protein family was discovered in the course of studies of signaling specificity from IFN receptors.[57] STAT3 is one of the seven members of the STAT protein family that mediates the actions of many cytokines and growth factors.[58] Recent data, especially from the analysis of conditional loss of STAT3 protein in adult tissues, confirm that STAT3 participates in various physiological processes and even directs seemingly contradictory responses.[59] The function of STAT3 has been extensively studied in cell culture systems. Nicolaidou et al[60] demonstrated that monocytes induced STAT3 activation in human BMSCs to promote osteoblast formation. Park et al[61] discovered that EGCG administration modulated collagen production and proliferation in fibroblasts through STAT3 signaling. Mikami et al[62] showed that siRNA knockdown of STAT3 resulted in a significant reduction of ALP activity in the BMSCs treated with dexamethasone and BMP-2. Other researchers found increased osteoblast-specific markers in STAT3 mRNA-downregulated osteoblasts.[63,64] Currently, the relationship between STAT3 and osteogenesis remains controversial.[60,62–64] EGCG is involved in various signaling pathways to modulate cellular responses.[61] In our study, 5 μM and 10 μM EGCG significantly decreased the phosphorylation of STAT3 and

significantly increased osteogenic marker expression. However, 1 μM EGCG had no substantial effect on the phosphorylation of STAT3 in hASCs. Therefore, we speculated that the STAT3 pathway might be involved in the EGCG-induced osteogenesis of hASCs.

Conclusion

In the present study, we demonstrated that EGCG enhanced osteogenic differentiation and suppressed adipogenesis in hASCs at 5 μM. EGCG has the potential to be used in hASC-based bone tissue engineering.

Acknowledgment

This work was supported by the National Natural Science Foundation of China (81400533 and 81671926), the Medical Scientific Research Project of Zhejiang Province (2015KYB146), and the Traditional Chinese Medicine Scientific Project of Zhejiang Province (2018ZQ034).

Disclosure

The authors report no conflicts of interest in this work.

References

1. Zhang X, Guo J, Zhou Y, Wu G. The roles of bone morphogenetic proteins and their signaling in the osteogenesis of adipose-derived stem cells. *Tissue Eng Part B Rev*. 2014;20(1):84–92. doi:10.1089/ten.TEB.2013.0204
2. Calori GM, Albisetti W, Agus A, Iori S, Tagliabue L. Risk factors contributing to fracture non-unions. *Injury*. 2007;38(Suppl 2):S11–S18.
3. Einhorn TA. Enhancement of fracture-healing. *J Bone Joint Surg Am*. 1995;77(6):940–956.
4. Tzioupis C, Giannoudis PV. Prevalence of long-bone non-unions. *Injury*. 2007;38(Suppl 2):S3–S9.
5. Quarto R, Mastrogiacomo M, Cancedda R, et al. Repair of large bone defects with the use of autologous bone marrow stromal cells. *N Engl J Med*. 2001;344(5):385–386. doi:10.1056/NEJM200102013440516
6. Kumar P, Vinitha B, Fathima G. Bone grafts in dentistry. *J Pharm Bioallied Sci*. 2013;5(Suppl 1):S125–S127. doi:10.4103/0975-7406.113312
7. O'Brien FJ. Biomaterials & scaffolds for tissue engineering. *Mater Today*. 2011;14(3):88–95. doi:10.1016/S1369-7021(11)70058-X
8. Wang Z, Zhang D, Hu Z, et al. MicroRNA-26a-modified adipose-derived stem cells incorporated with a porous hydroxyapatite scaffold improve the repair of bone defects. *Mol Med Rep*. 2015;12(3):3345–3350. doi:10.3892/mmr.2015.3795
9. Bianco P, Robey PG. Stem cells in tissue engineering. *Nature*. 2001;414(6859):118–121. doi:10.1038/35102181
10. Zuk PA, Zhu M, Mizuno H, et al. Multilineage cells from human adipose tissue: implications for cell-based therapies. *Tissue Eng*. 2001;7(2):211–228. doi:10.1089/107632701300062859
11. Fraser JK, Wulur I, Alfonso Z, Hedrick MH. Fat tissue: an underappreciated source of stem cells for biotechnology. *Trends Biotechnol*. 2006;24(4):150–154. doi:10.1016/j.tibtech.2006.01.010
12. Nakanishi C, Nagaya N, Ohnishi S, et al. Gene and protein expression analysis of mesenchymal stem cells derived from rat adipose tissue and bone marrow. *Circ J*. 2011;75(9):2260–2268.
13. Dmitrieva RI, Minullina IR, Bilibina AA, Tarasova OV, Anisimov SV, Zaritskey AY. Bone marrow- and subcutaneous adipose tissue-derived mesenchymal stem cells: differences and similarities. *Cell Cycle*. 2012;11(2):377–383. doi:10.4161/cc.11.2.18858
14. Levi B, Hyun JS, Nelson ER, et al. Nonintegrating knockdown and customized scaffold design enhances human adipose-derived stem cells in skeletal repair. *Stem Cells*. 2011;29(12):2018–2029. doi:10.1002/stem.757
15. Sheyn D, Pelled G, Zilberman Y, et al. Nonvirally engineered porcine adipose tissue-derived stem cells: use in posterior spinal fusion. *Stem Cells*. 2008;26(4):1056–1064. doi:10.1634/stemcells.2007-0858
16. Mehrkens A, Saxer F, Guven S, et al. Intraoperative engineering of osteogenic grafts combining freshly harvested, human adipose-derived cells and physiological doses of bone morphogenetic protein-2. *Eur Cell Mater*. 2012;24:308–319.
17. Shiraishi T, Sumita Y, Wakamastu Y, Nagai K, Asahina I. Formation of engineered bone with adipose stromal cells from buccal fat pad. *J Dent Res*. 2012;91(6):592–597.
18. Panetta NJ, Gupta DM, Lee JK, Wan DC, Commons GW, Longaker MT. Human adipose-derived stromal cells respond to and elaborate bone morphogenetic protein-2 during in vitro osteogenic differentiation. *Plast Reconstr Surg*. 2010;125(2):483–493.
19. Shen Q, Yu C, Guo Y, et al. Habitual tea consumption and risk of fracture in 0.5 million Chinese adults: a prospective cohort study. *Nutrients*. 2018;10(11). doi:10.3390/nu10111633.
20. Johnell O, Gullberg B, Kanis JA, et al. Risk factors for hip fracture in European women: the MEDOS study. Mediterranean osteoporosis study. *J Bone Miner Res*. 1995;10(11):1802–1815. doi:10.1002/jbmr.5650101125
21. Hegarty VM, May HM, Khaw KT. Tea drinking and bone mineral density in older women. *Am J Clin Nutr*. 2000;71:1003–1007. doi:10.1093/ajcn/71.4.1003
22. Khokhar S, Venema D, Hollman PC, Dekker M, Jongen W. A RP-HPLC method for the determination of tea catechins. *Cancer Lett*. 1997;114(1–2):171–172.
23. Nichols JA, Katiyar SK. Skin photoprotection by natural polyphenols: anti-inflammatory, antioxidant and DNA repair mechanisms. *Arch Dermatol Res*. 2010;302(2):71–83. doi:10.1007/s00403-009-1001-3
24. Fujiki H, Sueoka E, Watanabe T, Suganuma M. Synergistic enhancement of anticancer effects on numerous human cancer cell lines treated with the combination of EGCG, other green tea catechins, and anticancer compounds. *J Cancer Res Clin Oncol*. 2015;141(9):1511–1522. doi:10.1007/s00432-014-1899-5
25. Ramesh E, Elanchezhian R, Sakthivel M, et al. Epigallocatechin gallate improves serum lipid profile and erythrocyte and cardiac tissue antioxidant parameters in Wistar rats fed an atherogenic diet. *Fundam Clin Pharmacol*. 2008;22(3):275–284. doi:10.1111/j.1472-8206.2008.00585.x
26. Xu JZ, Yeung SY, Chang Q, Huang Y, Chen ZY. Comparison of antioxidant activity and bioavailability of tea epicatechins with their epimers. *Br J Nutr*. 2004;91(6):873–881. doi:10.1079/BJN20041132
27. Mereles D, Hunstein W. Epigallocatechin-3-gallate (EGCG) for clinical trials: more pitfalls than promises? *Int J Mol Sci*. 2011;12(9):5592–5603. doi:10.3390/ijms12095592
28. Chen CH, Ho ML, Chang JK, Hung SH, Wang GJ. Green tea catechin enhances osteogenesis in a bone marrow mesenchymal stem cell line. *Osteoporos Int*. 2005;16(12):2039–2045. doi:10.1007/s00198-005-1995-0
29. Wei YJ, Tsai KS, Lin LC, et al. Catechin stimulates osteogenesis by enhancing PP2A activity in human mesenchymal stem cells. *Osteoporos Int*. 2011;22(5):1469–1479. doi:10.1007/s00198-010-1352-9
30. Lin J, Della-Fera MA, Baile CA. Green tea polyphenol epigallocatechin gallate inhibits adipogenesis and induces apoptosis in 3T3-L1 adipocytes. *Obes Res*. 2005;13(6):982–990. doi:10.1038/oby.2005.115
31. Jin R, Shen M, Yu L, Wang X, Lin X. Adipose-derived stem cells suppress inflammation induced by IL-1beta through down-regulation of P2X7R mediated by miR-373 in chondrocytes of osteoarthritis. *Mol Cells*. 2017;40(3):222–229. doi:10.14348/molcells.2017.2314
32. Lou G, Song X, Yang F, et al. Exosomes derived from miR-122-modified adipose tissue-derived MSCs increase chemosensitivity of hepatocellular carcinoma. *J Hematol Oncol*. 2015;8:122. doi:10.1186/s13045-015-0220-7
33. Liu Y, Wu G, de Groot K. Biomimetic coatings for bone tissue engineering of critical-sized defects. *J R Soc Interface*. 2010;7(Suppl 5):S631–S647. doi:10.1098/rsif.2010.0115.focus

34. Zhang X, Jiang W, Liu Y, et al. Human adipose-derived stem cells and simvastatin-functionalized biomimetic calcium phosphate to construct a novel tissue-engineered bone. *Biochem Biophys Res Commun*. 2018; 495(1):1264–1270. doi:10.1016/j.bbrc.2017.11.150
35. Kaida K, Honda Y, Hashimoto Y, Tanaka M, Baba S. Application of green tea catechin for inducing the osteogenic differentiation of human dedifferentiated fat cells in vitro. *Int J Mol Sci*. 2015;16(12):27988–28000. doi:10.3390/ijms161226081
36. Zeng Q, Li X, Beck G, Balian G, Shen FH. Growth and differentiation factor-5 (GDF-5) stimulates osteogenic differentiation and increases vascular endothelial growth factor (VEGF) levels in fat-derived stromal cells in vitro. *Bone*. 2007;40(2):374–381. doi:10.1016/j.bone.2006.09.022
37. Knippenberg M, Helder MN, Zandieh Doulabi B, Wuisman PI, Klein-Nulend J. Osteogenesis versus chondrogenesis by BMP-2 and BMP-7 in adipose stem cells. *Biochem Biophys Res Commun*. 2006; 342(3):902–908. doi:10.1016/j.bbrc.2006.02.052
38. Al-Salleeh F, Beatty MW, Reinhardt RA, Petro TM, Crouch L. Human osteogenic protein-1 induces osteogenic differentiation of adipose-derived stem cells harvested from mice. *Arch Oral Biol*. 2008;53(10): 928–936. doi:10.1016/j.archoralbio.2008.05.014
39. Sokolsky-Papkov M, Agashi K, Olaye A, Shakesheff K, Domb AJ. Polymer carriers for drug delivery in tissue engineering. *Adv Drug Deliv Rev*. 2007;59(4–5):187–206. doi:10.1016/j.addr.2007.04.001
40. Yang CH, Lin CY, Yang JH, Liou SY, Li PC, Chien CT. Supplementary catechins attenuate cooking-oil-fumes-induced oxidative stress in rat lung. *Chin J Physiol*. 2009;52(3):151–159.
41. Sugisawa A, Umegaki K. Physiological concentrations of (-)-epigallocatechin-3-O-gallate (EGCg) prevent chromosomal damage induced by reactive oxygen species in WIL2-NS cells. *J Nutr*. 2002;132(7): 1836–1839. doi:10.1093/jn/132.7.1836
42. Yagi H, Tan J, Tuan RS. Polyphenols suppress hydrogen peroxide-induced oxidative stress in human bone-marrow derived mesenchymal stem cells. *J Cell Biochem*. 2013;114(5):1163–1173. doi:10.1002/jcb.24459
43. Jin P, Wu H, Xu G, Zheng L, Zhao J. Epigallocatechin-3-gallate (EGCG) as a pro-osteogenic agent to enhance osteogenic differentiation of mesenchymal stem cells from human bone marrow: an in vitro study. *Cell Tissue Res*. 2014;356(2):381–390. doi:10.1007/s00441-014-1797-9
44. Vali B, Rao LG, El-Sohemy A. Epigallocatechin-3-gallate increases the formation of mineralized bone nodules by human osteoblast-like cells. *J Nutr Biochem*. 2007;18(5):341–347. doi:10.1016/j.jnutbio.2006.06.005
45. Jin P, Liao L, Lin X, et al. Stimulating effect of a novel synthesized sulfonamido-based gallate ZXHA-TC on primary osteoblasts. *Yonsei Med J*. 2015;56(3):760–771. doi:10.3349/ymj.2015.56.3.760
46. Otto F, Thornell AP, Crompton T, et al. Cbfa1, a candidate gene for cleidocranial dysplasia syndrome, is essential for osteoblast differentiation and bone development. *Cell*. 1997;89(5):765–771.
47. Komori T. Regulation of bone development and maintenance by Runx2. *Front Biosci*. 2008;13:898–903.
48. Lee KS, Kim HJ, Li QL, et al. Runx2 is a common target of transforming growth factor beta1 and bone morphogenetic protein 2, and cooperation between Runx2 and Smad5 induces osteoblast-specific gene expression in the pluripotent mesenchymal precursor cell line C2C12. *Mol Cell Biol*. 2000;20(23):8783–8792.
49. Maruyama Z, Yoshida CA, Furuichi T, et al. Runx2 determines bone maturity and turnover rate in postnatal bone development and is involved in bone loss in estrogen deficiency. *Dev Dyn*. 2007;236(7):1876–1890. doi:10.1002/dvdy.21187
50. Lin L, Shen Q, Wei X, et al. Comparison of osteogenic potentials of BMP4 transduced stem cells from autologous bone marrow and fat tissue in a rabbit model of calvarial defects. *Calcif Tissue Int*. 2009; 85(1):55–65. doi:10.1007/s00223-009-9250-x
51. Lin YF, Jing W, Wu L, et al. Identification of osteo-adipo progenitor cells in fat tissue. *Cell Prolif*. 2008;41(5):803–812. doi:10.1111/j.1365-2184.2008.00542.x
52. Farmer SR. Transcriptional control of adipocyte formation. *Cell Metab*. 2006;4(4):263–273. doi:10.1016/j.cmet.2006.07.001
53. Siersbaek R, Nielsen R, Mandrup S. PPARgamma in adipocyte differentiation and metabolism – novel insights from genome-wide studies. *FEBS Lett*. 2010;584(15):3242–3249. doi:10.1016/j.febslet.2010.06.010
54. Linhart HG, Ishimura-Oka K, DeMayo F, et al. C/EBPalpha is required for differentiation of white, but not brown, adipose tissue. *Proc Natl Acad Sci U S A*. 2001;98(22):12532–12537.
55. Rosen ED, Hsu CH, Wang X, et al. C/EBPalpha induces adipogenesis through PPARgamma: a unified pathway. *Genes Dev*. 2002;16(1): 22–26. doi:10.1101/gad.948702
56. Tang W, Song H, Cai W, Shen X. Real time monitoring of inhibition of adipogenesis and angiogenesis by (-)-Epigallocatechin-3-gallate in 3T3-L1 adipocytes and human umbilical vein endothelial cells. *Nutrients*. 2015;7(10):8871–8886. doi:10.3390/nu7105437
57. Darnell Jr JE, Kerr IM, Stark GR. Jak-STAT pathways and transcriptional activation in response to IFNs and other extracellular signaling proteins. *Science*. 1994;264(5164):1415–1421.
58. Darnell Jr JE STATs and gene regulation. *Science*. 1997;277(5332): 1630–1635.
59. Levy DE, Lee CK. What does Stat3 do? *J Clin Invest*. 2002;109(9): 1143–1148. doi:10.1172/JCI15650
60. Nicolaidou V, Wong MM, Redpath AN, et al. Monocytes induce STAT3 activation in human mesenchymal stem cells to promote osteoblast formation. *PLoS One*. 2012;7(7):e39871. doi:10.1371/journal.pone.0039871
61. Park G, Yoon BS, Moon JH, et al. Green tea polyphenol epigallocatechin-3-gallate suppresses collagen production and proliferation in keloid fibroblasts via inhibition of the STAT3-signaling pathway. *J Invest Dermatol*. 2008;128(10):2429–2441. doi:10.1038/jid.2008.103
62. Mikami Y, Asano M, Honda MJ, Takagi M. Bone morphogenetic protein 2 and dexamethasone synergistically increase alkaline phosphatase levels through JAK/STAT signaling in C3H10T1/2 cells. *J Cell Physiol*. 2010;223(1):123–133. doi:10.1002/jcp.22017
63. Peruzzi B, Cappariello A, Del Fattore A, Rucci N, De Benedetti F, Teti A. c-Src and IL-6 inhibit osteoblast differentiation and integrate IGFBP5 signalling. *Nat Commun*. 2012;3:630. doi:10.1038/ncomms1651
64. Chipoy C, Berreur M, Couillaud S, et al. Downregulation of osteoblast markers and induction of the glial fibrillary acidic protein by oncostatin M in osteosarcoma cells require PKCdelta and STAT3. *J Bone Miner Res*. 2004;19(11):1850–1861. doi:10.1359/JBMR.040817